The Response Time of PMSE to Ionospheric Heating

E. Belova

Swedish Institute of Space Physics, Box 812, 98128 Kiruna, Sweden

P. B. Chilson

Cooperative Institute for Research in Environmental Sciences, University of Colorado, and NOAA Environmental Technology Laboratory, 325 Broadway, Boulder, Colorado 80305-3328, USA

S. Kirkwood

Swedish Institute of Space Physics, Box 812, 98128 Kiruna, Sweden

M. T. Rietveld

EISCAT, Ramfjordbotn, N-9027 Tromsdalen, Norway and Max-Plank-Institut für Aeronomie, D-37191 Katlenburg-Lindau, Germany

Abstract

During July of 1999, experiments were conducted in Northern Norway to investigate the effects of ionospheric heating on polar mesosphere summer echoes (PMSE). The experiments were conducted using the EISCAT VHF radar and the heating facility. It was shown that heating can dramatically reduce the backscattered echo power of PMSE. Here, we re-examine the high temporal resolution data of the PMSE backscattered power from three of the experiments as a function of ionospheric heating. Particular attention is paid to the transitions from the heater off to on and on to off states. The transition time of the PMSE echo power from high to low and low to high, respectively, is estimated in both cases to be less than 30 ms. It is suggested that enhancement of the electron diffusivity during heating is unlikely to account for such a fast decrease of radar backscattered power when the heater is switched on. We consider that an increase of the Debye length up to one sixth of a radar wavelength due to electron heating in the presence of aerosols might explain the observed heating effect on PMSE.

Introduction

The polar mesosphere/ionosphere plays host to a wide range of dynamic and chemical processes. There are breaking atmospheric waves, which deposit momentum and energy, precipitating energetic particles that affect the ion composition, and in the summer months, cold temperatures, which lead to aerosol formation. Furthermore, an understanding of the dynamical coupling between the upper mesosphere and lower thermosphere across the mesopause is complicated by the disparate physics that dominate in these two domains, especially at high latitudes (Hocking, 1996). Unfortunately, obtaining data from the polar mesopause region is difficult, which makes the data that we have all the more valuable when trying to unlock some of its mysteries.

The mesosphere-stratosphere-troposphere (MST) class of Doppler VHF radars has been a great asset in advancing our knowledge of the polar mesosphere. VHF radar signals are weakly backscattered from meter-scale irregularities of the refractive index, which at mesospheric altitudes are caused by fluctuations of electron density. The radar returns from these heights are particularly weak and are only detected from intermittently occurring layers of thin vertical extent. However, Ecklund and Balsley (1981) reported the observation of abnormally strong and persistent radar returns from the mesopause region (around 85 km altitude) above Alaska during the mid-summer months. This phenomenon has been termed polar mesosphere summer echoes (PMSE) (Röttger, et al, 1988), although they have also been observed at mid-latitudes (e.g., Reid, et al., 1989; Thomas, et al., 1992; Chilson, et al., 1997). Overviews of PMSE are given by Cho and Kelley (1993) and Cho and Röttger (1997).

The intriguing aspect of PMSE lies in the fact that traditional radar scattering theory cannot explain the large backscattered powers observed in connection with them. At mesospheric heights, radar signals are dominated by Bragg scatter, resulting from turbulent fluctuations of the free electrons. That is, the backscattered power is proportional to the Bragg wave vector of the three-dimensional refractive-index spectrum. In the inertial subrange, the three-dimensional spectrum decays as $k^{-11/3}$, where k is the wavenumber. The decay is much faster for wavenumbers within the dissipation range. Turbulent fluctuations near the mesopause generally exist at spatial scales that lie within the dissipation range for those frequencies used by MST radars. Near the mesopause, the ratio of the neutral atmospheric molecular diffusion rate ν and the electron diffusion rate D is typically close to one. This ratio is known at the Schmidt number, and is defined as $Sc = \nu / D$. However, when $Sc > 1$, Kelly et al. (1987) showed the Bragg match for MST radars occurs within an extension to the fluctuation spectrum that appears just beyond the viscous cutoff. In the viscous-convective subrange, the energy of the three-dimensional turbulence spectrum drops off as k^{-3}. The enhancement in the Schmidt number can be attributed to suppression of electron diffusivity in the presence of low mobile charged aerosols or dust particles (Cho et al, 1992).

Nevertheless, neutral turbulence as a source of electron density fluctuations cannot fully account for all types of PMSE. At least four non-turbulent mechanisms have been proposed to generate electron density fluctuations in the mesopause region (see for example the review by Cho and Röttger, 1997). Whatever the mechanism of PMSE generation, the fluctuations in electron density are being smoothed out by electron diffusion. Reduced electron diffusivity seems to play a significant role in both turbulent and non-turbulent theories of generation of PMSE. If neutral turbulence is responsible for PMSE, the aerosols are thought to reduce electron diffusivity and allow electron fluctuations to exist on smaller spatial scales than for the neutral gas. Constraints on electron diffusivity are included in almost all generation mechanisms proposed in the non-turbulent theories.

The EISCAT (European incoherent scatter) VHF radar located near Tromso has been used for PMSE observations in many experiments (e.g. Röttger et al., 1988, Röttger et al., 1990, Chilson et al., 2001, Goldberg et al., 2001). PMSE observed with this radar show similar features as observed with MST radar (Hoppe et al., 1988). The same site is the location of the EISCAT Heating facility and its powerful HF transmitter. Electromagnetic waves transmitted with this facility are capable of heating electrons in the ionosphere and thus modifying the plasma state (Rietveld et al., 1993). Through application of this method, electron temperatures at mesospheric heights can be increased by up to an order of magnitude (Belova et al., 1995).

The first successful joint PMSE/heating experiment was conducted during the summer of 1999. The experiment was motivated by the intention of influencing the electron temperature near the mesopause using the EISCAT Heating facility during a PMSE event. Some of the processes such as aerosol charging, electron diffusivity, which are likely important for PMSE generation, are dependent on the electron temperature. By analysing the reaction of PMSE to heating, we expected to obtain new information regarding the role of these processes in the formation of PMSE.

The effect of electron heating on PMSE power as measured with the EISCAT VHF radar was observed as a decrease when the heating facility was switched on (Chilson et al., 2000). We found also that the reaction time of the modulation in PMSE power to the heating was less than 2 seconds (Chilson et al., 2000). Such a quick response of PMSE to heating allowed us to suggest that increasing the electron diffusion might be responsible for the dissipation of

PMSE. Irregularities in electron density, which we detect as PMSE, can dissipate due to enhanced diffusion caused by the electron temperature increase. Rapp and Lübken (2000) have reported a theoretical study of diffusion in a multicomponent plasma under enhanced electron temperature conditions. According their calculations, for the case of $T_e=20 \cdot T_n$, where T_e and T_n are the electron and neutral temperature, respectively, and for a ratio of attached to free charge of 20, the diffusion decay time is about 0.1 s. In order to make more definitive conclusions further analysis of the experimental data is needed, which takes full advantage of the higher available temporal resolution.

We begin by reviewing the radar and heater parameters used during the experiment. Then data examples from three of the experiments are presented at a higher temporal resolution than was given in Chilson et al. (2000). Based on these results, a new mechanism in proposed as being responsible for the decay in PMSE power due to the heating.

Experimental configuration

The joint PMSE/heating experiment reported here was conducted at the EISCAT site near Tromso, Norway (69.58° N, 19.22° E) on July 9-11, 1999. The EISCAT VHF radar was used to detect PMSE and the EISCAT Heating facility to heat the ionosphere. A description of the experiment can be found in Chilson et al., 2000; however, we repeat some of the salient features here for the sake of convenience to the reader.

The EISCAT VHF radar was operated at a frequency of 224.0 MHz, which corresponds to a radar wavelength of 1.33 m. Pulses were transmitted with an inter-pulse period of 2.487 ms, and 12 samples were coherently averaged to produce a single complex (in-phase and quadrature) data point. This results in a time resolution of 29.85 ms. A total of 64 data points were stored as a single data record before writing the information to disk. The resulting dwell time was 1.88 s, but the data dump interval was 2 s. A technical description regarding the radar can be found in La Hoz et al. (1989).

The EISCAT heating facility is capable of transmitting powerful radio waves in the frequency range of 3.85 to 8 MHz (Rietveld et al., 1993). The facility was operated over a large range of configurations for the collective set of experiments, so the parameters are discussed on a case-by-case basis in the next section. The time intervals of heating that we discuss below were either 10 s or 20 s, i.e., both proportional to the dump interval of the radar. The heating on/off transitions were also synchronised to the radar's sampling interval start times. Later we will see that this was a disadvantage of the experimental arrangement.

Data analysis and results

In a previous study (Belova et al., 2001) it was shown that the effect of heating on PMSE depended strongly on the background level of the PMSE, which in turn showed high variability. To eliminate this effect we have here selected three time and height ranges with a fairly stable background level of PMSE and have analysed the data with a time resolution of 29.85 ms. These cases are denoted as exp01, exp04, and exp07. Here we have adopted the original experimental numbering as given in Chilson et al. (2000). The relevant heating parameters for these three cases are provided below.

Experiment 1 (exp01) was conducted on July 9, and we have chosen to use a 14-minute long data segment during the time interval of 22:29 – 22:43 UT. The heater was operated in the extraordinary mode (this is likewise true for the other 2 experiments considered) at a transmitting frequency of 4.04 MHz and with an effective radiated power (EPR) of 194 MW. The transmitted signals were directed vertically. The heater was switched on for 10 s and then switched off for 10 s, and this modulation pattern was repeated many times.

We use a 15-minute long data segment from experiment 4 (exp04), which took place on July 10. The time interval ran from 01:04 to 01:19 UT. The heater transmitted at a frequency of 5.423 MHz with an ERP of 629 MW. This was the highest value of ERP for all of the experiments. Again the heater was directed vertically, but for this experiment, the heater modulation pattern was 20 s on and 20 s off.

Finally, we consider a 5-minute long data segment from experiment 7 (exp07), which was carried out on July 10. The time interval in this case is 22:32 – 22:37 UT. The heater was operated at a frequency of 4.04 MHz with an ERP of 183 MW. This time the heater was left on for the entire time of the experiment. Modulation of the heating effect was accomplished by steering the heater beam 10 s in the vertical direction and then 10 s 16° off zenith towards the south. In the latter case, the heater does not illuminate the same volume as observed by the radar, so it can be considered as if the heater was off. Beam steering is implemented electronically using antenna array phase modulation within 0.2 ms, which is much shorter than the radar's data sampling rate of 30 ms. Therefore, from the perspective of the radar data, one can consider that the beam steering was accomplished almost instantaneously.

It was mentioned by Chilson et al. (2000) that the transmitted radar power was slightly reduced when the heater was on. Thus, radar backscattered power should be corrected for exp01 and exp04 to obtain the real heating effect in PMSE. However, from Figure 4 of Chilson et al. (2000), it is clear that the transmitted power was reduced only by about 10%. Figure 4 of Chilson et al. (2000) also exhibits a time constant in the transmit power corresponding to the activation of the heater of about 8 s. During the time of the 1999 experiment, the transmitter high voltage was smoothed digitally and the transmit power was calculated them. Therefore, the apparent time constant results from this smoothing process and actual variations in the transmitted power could have occurred on shorter time scale. However, we still only expect an average drop in transmit power of about 10%, which is less than the observed reduction in PMSE power that corresponded with the heating. Note that by leaving the heater on continuously as in experiment 4, one need not consider dips in the radar's transmit power as a function of the heater state.

The backscattered powers during those time intervals and heights chosen for analysis have first been separated relative to the heater state at the time of the observations, that is, relative to whether the heater was on or off. Outliers in the time-series data for the power were identified as being those occurring beyond three standard deviations of the mean calculated for every time interval chosen for analysis. The outliers were then removed from the time-series. The signals for all intervals corresponding to heater on or off states have been averaged in the following way. The first data point collected after the heater was turned on was averaged together with all of the other first data points. This is then likewise done for the subsequent points. An example of the average backscattered power obtained is presented in Figure 1, where the abscissa shows the time relative to heater being switched on (upper panel) or off (lower panel). Gaps of 0.12 s in every 2-second interval are clearly seen from the plots.

The temporal behaviour of the PMSE power for exp01, exp04, and exp07 are presented in Figures 2, 3 and 4, respectively. For each experiment there are 2 plots corresponding to the transitions of heater on to heater off and heater off to heater on. Time is shown along the abscissa and is measured in seconds from the beginning or from the end of a heater–on interval, depending on the sequence of the heater status. We show in the figure only 4-second intervals containing the most interesting region, i.e., when the heater is switched from on to off (or vice versa). Mean values and standard deviations obtained for the whole intervals of heater on and off are shown with solid and dashed lines, respectively.

The effect of heating on PMSE power is seen distinctly for all 3 experiments. The greatest reduction of PMSE power occurred as might be expected for exp04, when the heating was most powerful.

Discussion

First we consider the reaction time of the PMSE power to heating. Unfortunately, due to the data-sampling arrangement, there is a gap in the PMSE power data corresponding to the last 0.12 s of each heating-on or heating-off period. Consider, for example, exp04 and the sequence of heater on for 20 s and heater off for the next 20 s. A mean value of PMSE power for heater on interval is $1.9 \cdot 10^5$ (arbitrary units) with a standard deviation of $7 \cdot 10^4$. The corresponding quantities for the period when the heater was off are $1.8 \cdot 10^6$ and $7 \cdot 10^5$, respectively. One might reasonably expect that during the last 0.12 s of each 20 s period, the PMSE power would lie within the limits defined by the same mean and the same standard deviation as for the previous 19.88 s. The heater was switched off exactly at the time corresponding to the time mark of 20 s on the plot in Figure 3. The first data point was obtained 30 ms after this time, and the corresponding PMSE power at this moment has already increased to the PMSE background level. One can conclude that the time for the PMSE to react to heater switch-off is close to or less than our time resolution, i.e., 30 ms or less. Similar considerations apply for the opposite sequence, heater off – heater on, for exp04, and for both switching directions for exp01. The situation is not so clear for exp07 due to the smaller heating effect and relatively high standard deviation.

Close examination of the bottom panels in Figures 2, 3 and 4, which correspond to the sequence of heater off to heater on, reveals one further feature. The first data points obtained just 30 ms after heater switch-on have values higher than one standard deviation above the mean for the heater-on state. This could mean that the time constant for the transition from background to heated state is slightly longer than the time resolution of 30 ms. However, we cannot make a firm conclusion when considering only 3 data points (one for each experiment), since significant numbers (16%) of individual points in the time series will exceed one standard deviation above the mean by pure chance.

The estimates that we have obtained for the time for PMSE to react to heating seem to be much less than those which were suggested by Rapp and Lübken (2000) for electron diffusion. Hypothetically, for an electron temperature 20 times higher than the neutral temperature, the time scale for diffusion could be as small as 30 ms. For this, however, the ratio of attached to free charge in the plasma-aerosol medium considered by Rapp and Lübken (2000) must be 100 or even more. If this ratio is instead equal to 10, then the characteristic diffusion time would be about 0.3 s, i.e., it would be an order of magnitude longer than the reaction time that we obtain according to Figure 2. It is very difficult to determine how high the ratio may be. The general assumption of current PMSE theories (Cho et al., 1992, Klostermeyer, 1997) is that the ratio be more than unity. However, rocket measurements inside of PMSE region summarised by Rapp et al. (2002) in Tables 2 and 3 give the ratio as ranging from 0.3 up to 30. We will show further that altering aerosol charging due to heating takes too much time. Thus it cannot account for an increase of negative aerosol charge and decrease of charge of free electrons and hence, an increase of their ratio within 30 ms. Because there is no clear evidence for the ratio to be 100 or more under undisturbed (natural) PMSE conditions, we need to consider whether some mechanism other than diffusion can explain the very fast reaction of PMSE to heating.

One of the important parameters for the scatter of radio waves is the Debye length, which can be determined by formula:

$$\lambda_D=(\varepsilon_0\kappa_B T_e/N_e e^2)^{1/2}, \quad (1)$$

or

$$\lambda_D(cm)=6.9[T_e(K)/N_e(cm^{-3})]^{1/2}, \quad (2)$$

where ε_0 is the permittivity of free space, k_B is the Boltzmann constant, N_e is the free electron density, and e is the electronic charge. We now consider the effects of having the probing radar wavelength be larger and smaller than the Debye length. If $1/(k\lambda_D) << 1$, where k is radar wave number (this corresponds approximately to $\lambda/6 << \lambda_D$, where λ is radar wave length), then in a volume illuminated by incident radio wave with about the same phase, the electrons can be considered as individual charged particles moving according to their thermal velocity distribution. Scattering occurring under these conditions is that of the thermal fluctuations of the free electrons. This is termed Thomson scattering. In turn, if $1/(k\lambda_D) >> 1$, then the electrons illuminated by the radio wave with the same phase have to participate in plasma screening and hence, to follow thermal ion fluctuations and to participate in collective plasma motions. In the latter case, scattering of radio waves occurs on plasma irregularities and is called coherent.

PMSE is an example of coherent scattering. This is confirmed by the strength of the echoes and narrowness of the Doppler spectra (e.g., for EISCAT observations Röttger, et al, 1988). At the summer mesopause for the case of thermal equilibrium $T_e=T_n \sim 130K$ (Lübken, 1999). Assuming $N_e=500$ cm^{-3} we get $\lambda_D=3.5$ cm which is much smaller than λ for the EISCAT VHF radar. However, when we heat electrons their temperature can increase by a factor as large as 20 (Belova et al, 2001) that leads to an increase of the Debye length. Let us estimate a critical electron temperature T_c and density N_c for which λ_D becomes equal to 1/k for the case of the EISCAT VHF radar. From (2) we get:

$$N_c\,(\mathrm{cm}^{-3}) \approx 0.1\cdot T_c(\mathrm{K}). \qquad (3)$$

So, for an electron temperature of 2500 K (roughly 20 times the thermal equilibrium value), and if N_e is less than 250 cm^{-3}, the Debye length exceeds one sixth of a radar wavelength which implies Thomson scattering on individual electrons rather than on electron plasma irregularities. This might be the reason for the sharp drop in the PMSE power when we heat electrons strongly enough.

The question is whether these conditions are met during PMSE. When we heat electrons, it is expected that we likewise influence the aerosol charging process due to the temperature dependence of the capture rates of electrons by aerosols (Natanson, 1960). Belova et al. (2001) showed that initially negatively charged aerosols can capture more electrons for enhanced electron temperature causing an additional depletion of free electron density. One can roughly estimate a time constant of the capture process as $\tau \approx 1/(\nu \cdot N_a)$, where ν is the capture coefficient (aerosol capture rate per electron). Setting $\nu = 2\cdot 10^{-4}$ cm^3/s (Belova et al., 2001) and τ=30 ms gives $N_a \approx 1.6\cdot 10^5$ cm^{-3}. This number seems to be unrealistically high. Rapp et al. (2002) discussed all possible candidates for the ice condensation nuclei and concluded that maximum abundance is up to 10^4 cm^{-3}. However, for this value of N_a the process of electron density decrease due to the capture by aerosols would be 10 times longer, i.e., 0.3 s. Thus in 30 ms after initiating heating the electron density cannot change markedly.

Therefore, the problem remains as to whether it is possible to have a value of N_e less than 250 cm^{-3} during ordinary “non-heated” PMSE. Rapp et al. (2002) analysed PMSE data together with all available data on electron density measured by rocket-borne instruments. According to their Table 1, PMSE were not observed in 3 cases when the electron density was 100, 120 and 300 cm^{-3}. On the basis of such a scarce data set it is difficult to confirm or reject the possibility that PMSE can exist for electron densities as low as 250 cm^{-3}.

To estimate the electron density during our PMSE/heating experiments Belova et al. (2001) used a model for the lower ionosphere and the cosmic noise absorption data as an input parameter (see references therein). We should note that there were not any strong variations of the radio noise absorption during our experiments indicating quiet night-time conditions without any strong electron or proton precipitations. Model calculations give us an electron density value of about 100 cm^{-3} at the altitudes of PMSE. This means that for an electron temperature enhanced by up to 2500 K, the Debye length could be long enough, compare with the radar wavelength, to result in Thomson scattering.

Strictly speaking the Thomson scattering criterion requires that $k\lambda_D >> 1$. Coherent scattering in turn implies the opposite inequality, $k\lambda_D << 1$. Our estimate of critical electron density was obtained for the condition of $k\lambda_D = 1$. It is a transition region where neither of the criteria will work and no pure type of either scattering can be expected. Probably, both types of scatter occur to some extent. A proper consideration of electromagneric wave scattering under such conditions requires numerical modelling and analysis. We should note that although the PMSE power decreases when heating is initiated, it still remains at a level much higher than expected for Thomson scattered signals. This seems to indicate that we have passed through the realm for which $k\lambda_D<<1$ (for coherent scattering) and into a regime where $k\lambda_D \approx 1$.

If the proposed mechanism is the driving factor during heating, the characteristic time of the process would be determined by the time needed to heat or cool electrons. The time constant for cooling is usually several times larger than for heating; however, at a height of 80 km they are both less than 1 ms (Gurevich, 1978, Rietveld et al., 1986).

Conclusions

We have analysed here measurements of PMSE power sampled with high time resolution using the EISCAT VHF radar during ionospheric heating experiments. We have been able to determine an upper limit for the time required for PMSE power to respond to switching the heater on or off. Despite a gap in the data, we are able to conclude that this characteristic time is less than 30 ms, which was the time resolution of the radar data recorded during the experiments. We believe that this time is too short to be accounted for by the effect of ionospheric heating on electron diffusion. Therefore, we propose another explanation for the heating effect on PMSE. During heating the electron temperature at PMSE heights is expected to grow significantly on a time scale of less than 1 ms. Increased electron temperature leads to an increase of the Debye length in the plasma. The Debye length can exceeds one sixth of the radar wavelength if electron density is low enough. Then the radar wave scattering will change from being coherent scatter from plasma irregularities to Thomson scatter from the individual electrons, and the backscattered signal power will fall. The time constant for this process is expected to be in the 1 ms range.

To determine more accurately the time constant of PMSE's response to heating more experiments are needed. The next experiment should be arranged in such a way that there are no gaps in data around the times of heater switch-on or switch-off. It would also be advisable to have a higher time resolution. This could give us more information to allow firmer conclusions regarding the processes responsible for the heating effect on PMSE.

Acknowledgments. The EISCAT Scientific Association is funded by SA (Finland), CNRS (France), MPG (Germany), NIPR (Japan), RCN (Norway), NFR (Sweden), and PPARC (UK).

References

Belova E.G., A.B. Pashin, and W.B. Lyatsky, Passage of powerful HF radio wave through the ionosphere as a function of initial electron density profiles. *J. Atmos. Terr. Phys., 57*, 265-272, 1995.

Belova, E., P.B. Chilson, M. Rapp, and S. Kirkwood, Electron temperature dependence of PMSE power: Experimental and modelling results, *Advances in Space Research*, *28*, 7, 1077-1082, 2001.

Chilson, P. B., P. Czechowsky, J. lostermeyer, R. Rüster, and G. Schmidt, An investigation of measured temperature profiles and VHF mesosphere summer echoes at midlatitudes, *J. Geophys. Res.*, *102,* 23819-23828, 1997.

Chilson, P.B., E. Belova, M.T. Rietveld, S. Kirkwood and U.-P. Hoppe, First artificially induced modulation of PMSE using the EISCAT heating facility, *Geophys. Res. Lett*., *27,* 3801-3804, 2000.

Chilson, P.B., S. Kirkwood, and I. Häggström, Frequency domain interferometry mode observations of PMSE using the EISCAT VHF radar, *Ann. Geophys., 18,* 1599-1612, 2001.

Cho, J. Y. N. and M. C. Kelley, Polar mesosphere summer radar echoes: Observations and current theories, *Rev. Geophys.*, *31,* 243-265, 1993.

Cho, J. Y. N. and J. Röttger, An updated review of polar mesosphere summer echoes: Observation, theory, and their relationship to noctilucent clouds and subvisible aerosols, *J. Geophys. Res.*, *102,* 2001-2020, 1997.

Ecklund, W. L. and B. B. Balsley, Long-term observations of the arctic mesopause with the radar at Poker Flat, Alaska, *J. Geophys. Res.*, *86,* 7775-7780, 1981.

Goldberg, R.A. et al., Dropps: A study of the polar summer mesosphere with rocket, radar and lidar, Geophys.Res. Lett, *28,* 1407-1410, 2001.

Gurevich, A.V., Nonlinear phenomena in the ionosphere, Springer-Verlag, 1978.

Hocking, W. K., Dynamical coupling processes between the middle atmosphere and lower ionosphere, *J. Atmos. Terr. Phys., 58,* 735-752, 1996.

Hoppe, U.-P., C.Hall; and J. Röttger; First observations of summer polar mesosheric backscatter with a 224-MHz radar, *Geophys. Res. Lett.*, *15,* 28-31, 1988.

Kelley, M. C., D. T. Farley, and J. Röttger, The effects of cluster ions on anomalous VHF backscatter from the summer polar mesosphere, *Geophys. Res. Lett., 14,* 1031-1034, 1987.

Klostermeyer, J., A height- and time-dependent model of polar mesosphere summer echoes, *J. Geophys. Res.*, *102,* 6715-6727, 1997.

La Hoz, C., J. Röttger, M. Rietveld, G. Wannberg, and S. J. Franke, The status and planned development of EISCAT in mesosphere and D-region experiments, *Handbook for MAP*, 28, SCOSTEP Secr., Univ. of Ill., Urbana, 476-488, 1989.

Lübken, F.-J., Thermal structure of the Arctic summer mesosphere, *J. Geophys. Res*., *104,* 9135-9149, 1999.

Natanson, G. L., On the theory of the charging of microscopic aerosol particles as a result of capture of gas ions, *Sov. Phys. Tech. Phys.* (engl. Transl.), **5**, 538-551, 1960.

Rapp, M., and F.-J. Lübken, Electron temperature control of PMSE, *Geophys. Res. Lett., 27,* 3285-3288, 2000.

Rapp, M., J. Gumbel, F.-J. Lübken, and R. Latteck, D-region electron number density limits for the existence of polar mesosphere summer echoes, accepted for publication in *J. Geophys. Res*., January 2002.

Reid, I. M., P. Czechowsky, R. Rüster, and G. Schmidt, First VHF radar measurements of mesopause summer echoes at mid-latitudes, *Geophys. Res. Lett.*, *16*, 135-138, 1989.

Rietveld, M. T., H. Kopka, and P. Stubbe, D-region characteristics deduced from pulsed ionospheric heating under auroral electrojet conditions, J. Atmos. Terr. Phys., *48,* 311-326, 1986.

Rietveld, M. T., H. Kohl, H. Kopka, and P. Stubbe, Introduction to ionospheric heating at Tromso - I. experimental overview, *J. Atmos. Terr. Phys*., *55,* 577-599, 1993.

Röttger, J., C. La Hoz, M. C. Kelley, U.-P. Hoppe, and C. Hall, The structure and dynamics of polar mesosphere summer echoes observed with the EISCAT 224 MHz radar, *Geophys. Res. Lett.*, *15,* 1353-1356, 1988.

Röttger, J., C. La Hoz, C.J. Franke, and C.H. Liu, Steepening of reflectivity structures detected in high-resolution Doppler spectra of polar mesosphere summer echoes (PMSE) observed with the EISCAT 224-MHz radar, J. Atmos. Terr. Phys., *52,* 939-954, 1990.

Thomas, L., and I. Astin, and T. Prichard, The characteristics of VHF echoes from the summer mesopause region at mid-latitudes, *J. Atmos. Terr. Phys.*, *54,* 969-977, 1992.

Figure captions.

Figure 1:

Examples of the transition in averaged PMSE backscattered power as a function of electron heating. Transition in the state of the heater from one to off and off to on are depicted in the upper panel and lower panel, respectively. Measurements used for both examples are taken for the same height.

Figure 2:

Examples of the transition in averaged PMSE backscattered power as a function of electron heating for experiment 1. The state of the heater is indicated. Mean values and standard deviations of the measurements are shown with solid and dashed lines, respectively. See text for additional information.

Figure 3:

The same as in Figure 2 but for experiment 4.

Figure 4:

The same as in Figure 2 but for experiment 7.

Figure 1.

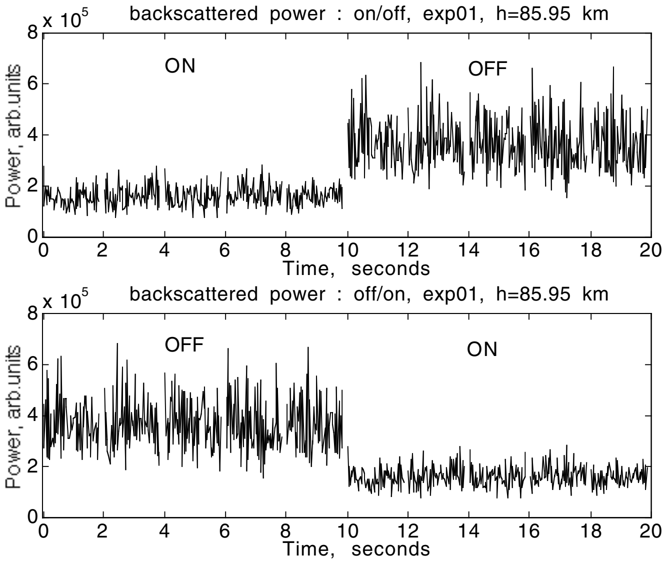
backscattered power : on/off, exp01, h=85.95 km
x 10^5
Power, arb.units
ON
OFF
0
2
4
6
8
Time, seconds
0
2
4
6
8
10
12
14
16
18
20
backscattered power : off/on, exp01, h=85.95 km
x 10^5
Power, arb.units
OFF
ON
0
2
4
6
8
Time, seconds
0
2
4
6
8
10
12
14
16
18
20

Figure 2.

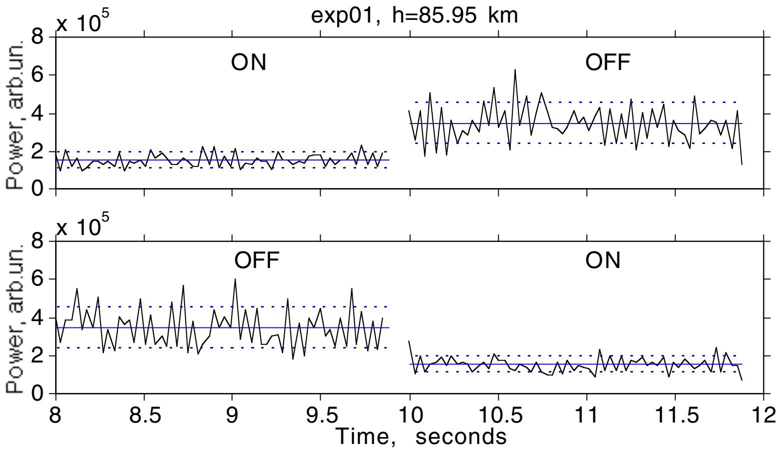
exp01, h=85.95 km
x 10^5
Power, arb.un.
8
6
4
2
0
ON
OFF
x 10^5
Power, arb.un.
OFF
ON
8
8.5
9
9.5
10
10.5
11
11.5
12
Time, seconds

Figure 3

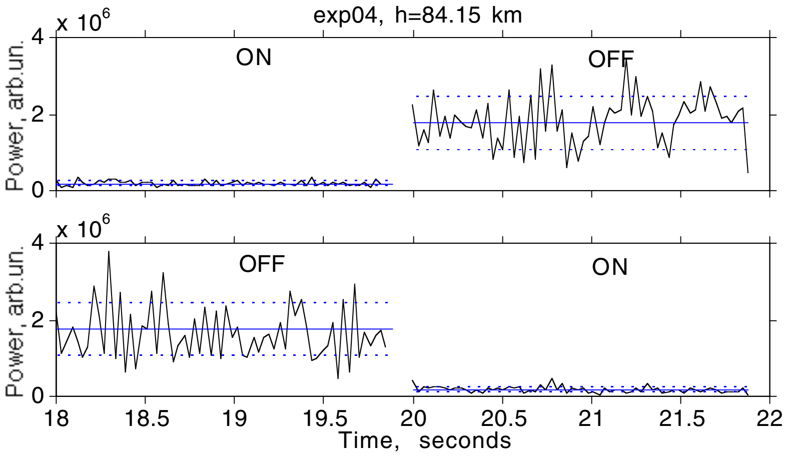
exp04, h=84.15 km
x 10^6
Power, arb.un.
ON
OFF
4
2
0
x 10^6
Power, arb.un.
OFF
ON
4
2
0
18
18.5
19
19.5
20
20.5
21
21.5
22
Time, seconds

Figure 4.

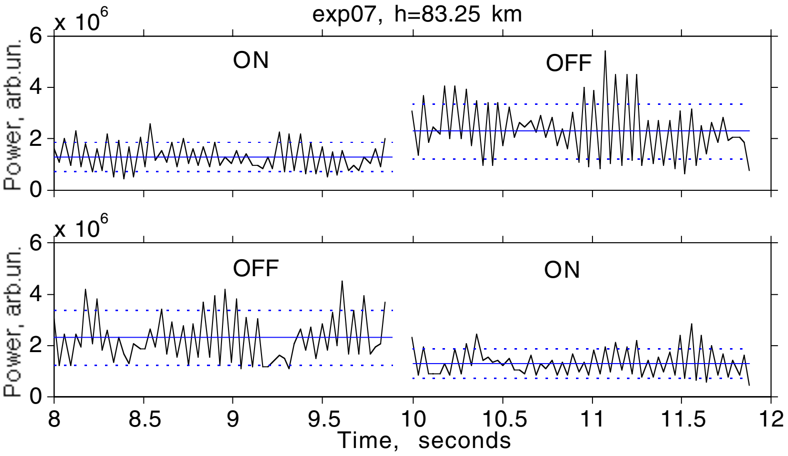
exp07, h=83.25 km
x 10^6
Power, arb.un.
ON
OFF
x 10^6
Power, arb.un.
OFF
ON
0
2
4
6
8
8.5
9
9.5
10
10.5
11
11.5
12
Time, seconds